

Global net community production estimated from the annual cycle of surface water total dissolved inorganic carbon

Kitack Lee¹

Cooperative Institute of Marine and Atmospheric Study, University of Miami, c/o Atlantic Oceanographic and Meteorological Laboratory/NOAA, Miami, Florida 33149

Abstract

Global net community production is determined, for the first time, from the decrease in salinity (S)-normalized total dissolved inorganic carbon ($NC_T = C_T \times 35/S$) inventory in the surface mixed layer corrected for changes due to net air-sea CO_2 exchange and diffusive carbon flux from the upper thermocline. Changes in the mixed layer NC_T inventory are estimated using a derived annual cycle of NC_T and global records of the mixed layer depth. The annual NC_T cycle is deduced from regional algorithms relating NC_T to sea surface temperature (SST) and nitrate (NO_3^-), along with global records of seasonal mean SST and NO_3^- , and from the monthly mean surface partial pressure of CO_2 and total alkalinity fields using thermodynamic models. The two methods show similar regional trends and yield global net community production estimates of 6.7 and 8.0 Gt C (1 Gt C = 1×10^{12} kg carbon), respectively. The two global estimates are not significantly different and represent an 8-month period of 1990 (warming period) during which the mixed layer NC_T concentration decreases. However, the estimates do not account for net community production during a 4-month cooling period. Ratios of net community production during the warming and cooling periods are estimated from multiyear sediment trap data at the Hawaii Ocean Time-series (22°N, 158°W) and Ocean Weather Station P (50°N, 145°W) sites. Global extrapolation of these ratios yields annual rates of net community production of 9.1 ± 2.7 and 10.8 ± 2.7 Gt C yr⁻¹.

Net community production in the euphotic zone of the ocean occurs when primary production is greater than community respiration. In a steady state, it is quantitatively equivalent to export production, which is the amount of organic carbon exported from the euphotic zone (Berger et al. 1987), and new production, which is the fraction of total primary production associated with newly available nitrate and dinitrogen gas (Dugdale and Goering 1967). The only way net community production (or export and new production) can play a direct role in oceanic uptake of anthropogenic CO_2 is if it changes with future climate variations (Falkowski et al. 1998). Thus, accurate estimates of net community production and its variations with time are important requirements for ocean biogeochemical studies (Falkowski et al. 1998).

Over seasonal to annual time-scales, net community pro-

duction can be estimated using mass balances of nutrients and dissolved gases in the mixed layer. Numerous studies have demonstrated that seasonal variations in the concentration of nutrients and oxygen in the mixed layer, coupled with Redfield ratio conversions, provide powerful tracers for estimating space and time integrated net community production (Jenkins and Goldman 1985; Jenkins and Wallace 1992; Emerson et al. 1997).

The biologically mediated decrease of salinity (S)-normalized total dissolved inorganic carbon concentration ($NC_T = C_T \times 35/S$) (ΔNC_T in mol C m⁻³) in the mixed layer is caused by the net production of organic carbon in both particulate and dissolved forms (E_{POC} and E_{DOC} , respectively) and particulate inorganic carbon (E_{PIC}) as $CaCO_3$, with the latter being much smaller:

$$\Delta NC_T = E_{POC} + E_{DOC} + E_{PIC} + A_{DOC}. \quad (1)$$

The ΔNC_T also accounts for a fraction of dissolved organic carbon accumulating in the mixed layer (A_{DOC}), if any.

The objective of this work is to determine global net community production using the mass balance of NC_T in the mixed layer. Since net community production does not include net $CaCO_3$ production (E_{PIC}), E_{PIC} is independently estimated using the mass balance of salinity (S)-normalized total alkalinity concentration ($NA_T = A_T \times 35/S$) in the mixed layer and, subsequently, subtracted from the total change in the mixed layer NC_T concentration. Maps of global net community and $CaCO_3$ production in the mixed layer presented in this paper can be useful in evaluating and improving three-dimensional models simulating the global carbon cycle in the ocean.

Data analysis and calculation methods

Analysis of surface C_T data—Derived regional NC_T algorithms: The method and global-scale C_T data used to de-

¹ Current address: Pohang University of Science and Technology/School of Environmental Science and Engineering, San 31, Hyojadong, Nam-gu, Pohang 790–784, Republic of Korea.

Acknowledgements

This paper benefited a great deal from the numerous constructive suggestions by Andre Morel and two anonymous reviewers. I am much indebted to R. Wanninkhof for his encouragement in carrying out this research and helpful comments on the manuscript. Discussions with R. Barber, P. Falkowski, D. Karl, R. Najjar, and J. Sarmiento were extremely helpful in the early stages of this work. Special thanks are further extended to D. Karl and E. Laws for providing me with their unpublished manuscripts. I would also like to thank Hee-Sook Kang of the Rosenstiel School of Marine and Atmospheric Science for preparing the color plates. This research was sponsored by the National Oceanic and Atmospheric Administration Office of Global Programs under grant GC99-156 (awarded to K.L.). The work was carried out under the auspices of the Cooperative Institute of Marine and Atmospheric Studies of the University of Miami.

rive regional algorithms are described in detail elsewhere (Lee et al. 2000). Changes in surface NC_T concentration are caused by net community production, net air-sea CO_2 exchange, and lateral and vertical mixing of water with different levels of NC_T . Net community production dominates the other processes when the mixed layer shoals during the warming period. As the season progresses, this net community production occurs in tandem with sea surface temperature (SST) increase and can be quantified by decreasing NC_T concentration in the mixed layer. Thus, changes in surface NC_T concentration are directly correlated with SST, but trends often differ geographically. Lee et al. (2000) suggest that the distribution of surface NC_T could be derived by dividing the world's oceans into five regions using a total of 12 equations relating NC_T to SST for areas between $30^\circ N$ and $30^\circ S$ or to SST and nitrate (NO_3^-) for areas $>30^\circ$.

Annual cycle of surface NC_T : The annual cycles of global surface NC_T used in this paper were published in Lee et al. (2000). The seasonal mean distribution of global surface NC_T was constructed from regional $NC_T/SST/NO_3^-$ algorithms, along with seasonal mean SST and NO_3^- fields for 1990 from the National Centers for Environmental Prediction/National Center for Atmospheric Research (NCEP/NCAR) reanalysis (Kalnay et al. 1996) and from the World Ocean Atlas 1998 (Conkright et al. 1998), respectively. An alternate way to estimate the annual cycle of C_T is to use monthly mean surface pCO_{2SW} and A_T fields. Monthly mean values of pCO_{2SW} were calculated using climatological ΔpCO_2 , the difference between pCO_{2SW} and pCO_{2AIR} (Takahashi et al. 1997), and the partial pressure of CO_2 in air, pCO_{2AIR} , for 1990 (Conway et al. 1994). Monthly mean global A_T fields were estimated from the regional NA_T algorithms, along with monthly mean SST and S fields (Lee et al. 2000). In this calculation, the monthly mean global distribution of C_T on 4° latitude \times 5° longitude grid cells was constructed from pCO_{2SW} and A_T fields using the carbonic acid dissociation constants of Mehrbach et al. (1973), as refit by Dickson and Millero (1987). The resulting C_T fields were then converted to NC_T using monthly mean S fields.

A mixed layer model to estimate net community production: Net community production in the mixed layer during the warming period of 1990, NCP_{ML-W} , is estimated from changes in the mixed layer NC_T inventory corrected for changes due to net air-sea CO_2 flux and advective and diffusive carbon flux from the upper thermocline in the following manner (Fig. 1):

$$\begin{aligned} NCP_{ML-W}|_{\Delta M} = & (AH^{M+1}[NC_T^M - NC_T^{M+1}]) \\ & + A(F_{air-sea})_{M+1} + AH^{M+1}W(dC_T/dm) \\ & + AK_V(dC_T/dm), \end{aligned} \quad (2)$$

where M denotes month or season (time step); A is the area of each grid cell; $[NC_T^M - NC_T^{M+1}]$ is the change in the NC_T concentration in the mixed layer, H ; F ($\text{mol m}^{-2} \text{month}^{-1}$) is the net air-sea CO_2 flux; W (m month^{-1}) and K_V ($\text{m}^2 \text{month}^{-1}$) are the advective velocity and diffusivity across

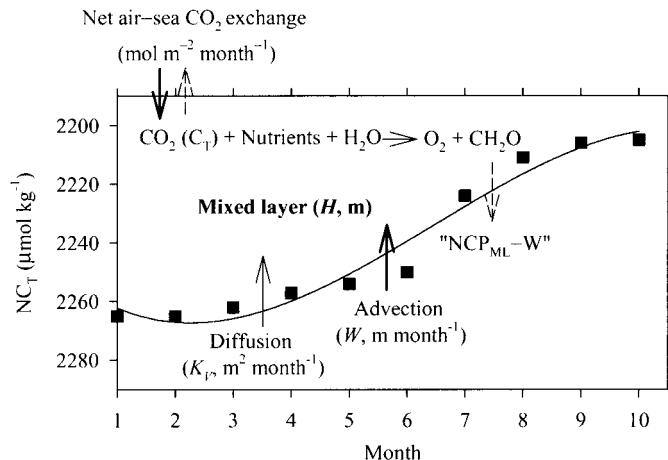


Fig. 1. Schematic diagram showing factors influencing mass balance of NC_T in the mixed layer. A solid line is best fit of the mean annual trend of the mixed layer NC_T concentration representing the North Pacific. The change in the mixed layer NC_T inventory during the warming period is determined by net community (NCP_{ML-W}), net air-sea CO_2 exchange, and vertical carbon flux via diffusion (K_V) and advection (W).

the bottom of the mixed layer, respectively; and dC_T/dm (mol m^{-4}) is the vertical gradient in the C_T concentration between the mixed layer and the upper thermocline. Global records of monthly or seasonal mean mixed layer depth used in this study are available at the National Oceanographic Data Center (<http://www.nodc.gov/oc5/mixdoc.html>). They are computed from climatological monthly or seasonal mean profiles of potential temperature and potential density (σ_θ) using the following criteria: a temperature change of $0.5^\circ C$ or a density change of 0.125 in σ_θ from the ocean surface (Monterey and Levitus 1997). The mixed layer depth fields are interpolated to $4^\circ \times 5^\circ$ grid cells to match the grid size used in the NC_T climatology.

Limited studies suggest that the evolution of mixed layer temperature can be adequately modeled by neglecting vertical advection of water when the mixed layer shoals (Denman and Miyake 1973). If this assumption holds true for much of the oceans, Eq. 2 reduces to

$$\begin{aligned} NCP_{ML-W}|_{\Delta M} = & (AH^{M+1}[NC_T^M - NC_T^{M+1}]) \\ & + A(F_{air-sea})_{M+1} + AK_V(dC_T/dm). \end{aligned} \quad (3)$$

It is conceivable, although difficult to quantify, that sporadic mixed layer deepening during the warming period could bring subsurface waters with higher NC_T to the surface and thus counteract the decrease of NC_T resulting from net community production. Surface horizontal advection is assumed to be insignificant in this calculation.

The three terms in Eq. 3 are calculated using monthly or seasonal mean inputs on each 4° latitude \times 5° longitude grid cell in which the mixed layer NC_T concentration decreases. The period for calculation is, on average, 8 months. Calculation for each component in Eq. 3 is presented below in detail.

Net change in the mixed layer NC_T inventory, $AH^{M+1}[NC_T^M - NC_T^{M+1}]$: The mixed layer NC_T concentration

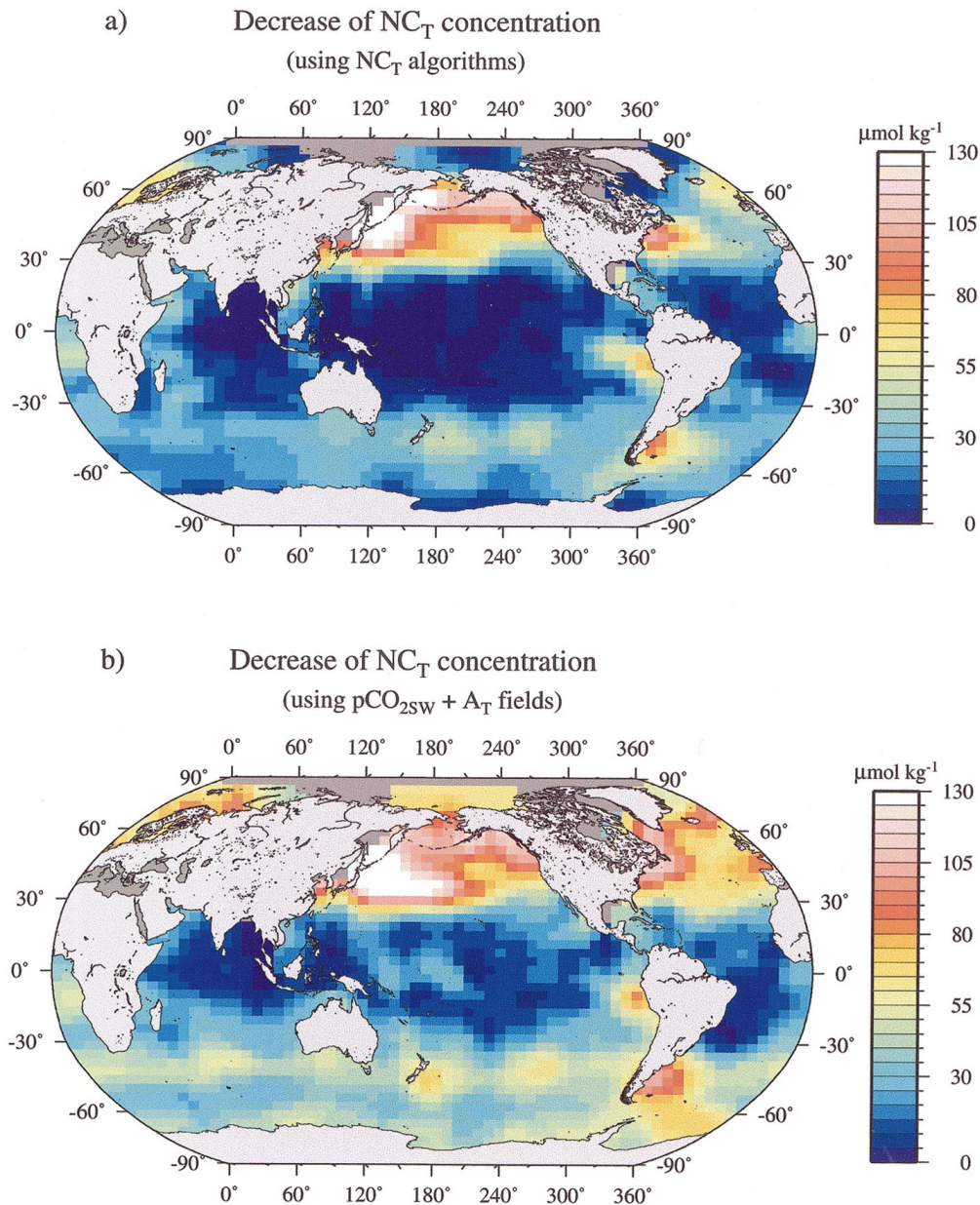


Fig. 2. Maps of the cumulative decrease in the mixed layer NC_T concentration derived from (a) regional NC_T /SST/ NO_3^- algorithms combined with seasonal mean SST for 1990 from the NCEP/NCAR reanalysis (Kalnay et al. 1996) and seasonal mean NO_3^- fields from the World Ocean Atlas (Conkright et al. 1998), and (b) from the $\text{pCO}_{2\text{sw}}$ (Takahashi et al. 1997) and A_T (Millero et al. 1998) fields using the carbonic acid dissociation constants of Mehrbach et al. (1973), as refit by Dickson and Millero (1987). Global records of seasonal mean NO_3^- are interpolated to a 4° latitude \times 5° longitude grid cell to match with the grid size used in the $\text{pCO}_{2\text{sw}}$ climatology.

is highest in the winter when deep convective mixing brings NC_T -rich water to the surface and lowest in the summer due to net community production. Maps depicting the decrease of surface NC_T concentration are approximately comparable to geographic patterns of net community production (Fig. 2).

The net change of the monthly and seasonal mean NC_T inventory in the mixed layer is determined on each grid cell using a derived annual NC_T cycle and mixed layer fields. The two methods used to derive the annual NC_T cycle yield

a global decrease of the mixed layer NC_T inventory of 5.8 and 7.1 Gt C. These global estimates are subject to errors due to uncertainties in the following sources: (1) Uncertainty of $\pm 10 \mu\text{mol kg}^{-1}$ in derived NC_T values (Lee et al. 2000); this is equivalent to an error of ± 2.1 Gt C; and (2) The mixed layer depth (Monterey and Levitus 1997). The global value of the mixed layer NC_T decrease calculated using temperature-based mixed layer depth fields is 0.7 Gt C higher than that using density-based fields used in this study. An

Table 1. Regional estimates of net community production (NCP) in the mixed layer during the warming period of 1990 (NCP_{ML}-W) (Gt C).

Ocean	Region	Area ($\times 10^{12}$ m ²)	Net air-sea CO ₂ flux (Gt C)	CIC _{ML} * NC _T † (Gt C)	CIC _{ML} A _T + pCO _{2SW} ‡ (Gt C)	Diffusive carbon flux (Gt C)	NCP _{ML} -W	NCP _{ML} -W
							NC _T (Gt C)	A _T + pCO _{2SW} (Gt C)
Atlantic	40°N–70°N	12.4	0.35	0.40	0.47	0.02	0.64 (0.76)	0.71 (0.83)
	40°N–40°S	49.1	–0.01	0.68	0.66	0.07	0.61 (0.75)	0.59 (0.73)
	South of 40°S	18.5	0.24	0.50	0.76	0.05	0.71 (0.79)	0.97 (1.05)
Indian	North of 40°S	43.3	0.02	0.44	0.50	0.08	0.46 (0.54)	0.52 (0.60)
	South of 40°S	23.4	0.16	0.51	0.84	0.06	0.63 (0.73)	0.96 (1.06)
Pacific	40°N–70°N	14.1	0.13	0.81	0.51	0.09	0.98 (1.03)	0.68 (0.73)
	40°N–40°S	119	–0.30	1.40	1.84	0.45	1.42 (1.55)	1.86 (1.99)
	South of 40°S	35	0.23	1.00	1.40	0.09	1.15 (1.32)	1.55 (1.72)
Arctic	North of 70°N	2.7	0.07	0.08	0.11	0.00	0.14 (0.16)	0.17 (0.19)
	Global	317.5	0.9	5.8	7.1	0.9	6.7§ (7.6) 	8.0 (8.9)

* CIC_{ML} (carbon inventory change) is the total decrease of the mixed layer NC_T inventory.

† CIC_{ML} estimated using the mixed layer NC_T decrease that are calculated from regional NC_T/SST/NO₃[–] algorithms along with seasonal mean SST and NO₃[–] fields.

‡ CIC_{ML} estimated using the mixed layer NC_T decrease that are calculated from the monthly mean pCO_{2SW} and A_T fields using the carbonic acid dissociation constants of Mehrbach et al. (1973), as refit by Dickson and Millero (1987).

§ NCP_{ML}-W corrected for CaCO_{3ML}-W as shown in Table 2.

|| NCP_{ML}-W in brackets includes CaCO_{3ML}-W.

error of ± 0.4 Gt C can thus be caused by uncertainties in the mixed layer depth fields, although the magnitude of the error may vary geographically. Overall, global estimates of the total decrease of the mixed layer NC_T inventory are subject to an error of up to ± 2.5 Gt C.

Net air-sea CO₂ exchange, $A(F_{\text{air-sea}})_{M+1}$: The monthly mean net CO₂ flux (mol m^{–2} month^{–1}) for each grid cell is calculated from global $\Delta p\text{CO}_2$ fields constructed by Takahashi et al. (1997), along with wind speed fields and the gas exchange velocity of Wanninkhof (1992) formulated for long-term winds. Oceanic CO₂ uptake (positive sign) counteracts the mixed layer NC_T decrease resulting from net community production, whereas efflux (negative sign) reinforces it. Net air-sea CO₂ flux in most of the oceans, except in the eastern equatorial Pacific, counteracts the mixed layer NC_T decrease, but its magnitude varies geographically ranging from 40% of the net community production in the North Atlantic to 20% or less in other regions (Table 1). The globally integrated net air-sea CO₂ flux during the warming period is about 0.9 Gt C, which is subject to an error of up to 50%, depending on the choice of relationships between gas exchange and wind speed.

Diffusive carbon flux, $A K_V dC_T/dm$: The diffusive flux of C_T from the top of the thermocline also counteracts the mixed layer NC_T decrease due to net community production. The monthly mean diffusive C_T flux is estimated on each grid cell using a regionally varying vertical C_T gradient representing the grid cell and K_V of 0.5×10^{-4} m² s^{–1}. The mean vertical C_T gradients representing five different regions as defined in Lee et al. (2000) range from 0.1 mmol C m^{–4} (increasing concentration with depth) in the subtropical Atlantic to 1 mmol C m^{–4} in the North Pacific.

The K_V of 0.5×10^{-4} m² s^{–1} combined with regional mean vertical C_T gradients yields a global diffusive flux of 0.9 Gt C, which accounts for about 10% of the global estimates of

net community production (Table 1). Sensitivity studies are performed by using acceptable values of K_V ranging from 0.1 to 1×10^{-4} m² s^{–1} (Munk 1966; Ledwell et al. 1993) in such a way as to estimate the possible maximum and minimum values of diffusive C_T flux. The K_V of 0.1×10^{-4} m² s^{–1} has little effect on the mixed layer NC_T inventory, but the K_V of 1×10^{-4} m² s^{–1} yields a diffusive flux of 1.8 Gt C. Thus, the global diffusive C_T flux of 0.9 Gt C during the warming period has an error of ± 0.9 Gt C.

Analysis of surface A_T data—Derived regional NA_T algorithms and annual cycle of surface NA_T: The method and global-scale A_T data used to derive regional NA_T/SST algorithms are described in Millero et al. (1998). In the open ocean the processes that can change NA_T in a measurable way are CaCO₃ formation and dissolution (Ca²⁺ + 2HCO₃[–] ↔ CaCO₃ + H₂O + CO₂) and NO₃[–] uptake and regeneration (Brewer et al. 1975). The removal of NO₃[–] to form organic matter raises NA_T of surface waters, partly compensating for decrease in NA_T resulting from CaCO₃ formation. Thus, net CaCO₃ production (CaCO_{3ML} in mol C m^{–3}) is obtained taking half of the NO₃[–] corrected NA_T changes:

$$\text{CaCO}_{3\text{ML}} = (\Delta\text{NA}_T + \Delta\text{NO}_3^-) \times 0.5, \quad (4)$$

where the sum of ΔNA_T and ΔNO_3^- is $\Delta\text{A}_{\text{POT}}$. The global distribution of surface NA_T shows that the major ocean basins can be divided into six regions where different trends of NA_T are observed, and boundaries between the regions are similar to those of large-scale ocean currents (Millero et al. 1998). The NA_T in (sub)tropical waters with temperatures $>20^\circ\text{C}$ is invariant except in upwelling areas. The NA_T increases toward high latitudes ($>30^\circ$) and is inversely proportional to SST. Seasonal mean NA_T fields are constructed from regional NA_T/SST algorithms and the global records of SST to match the temporal resolution used in the NO₃[–] fields (Lee et al. 2000). Estimated NA_T fields are then combined with NO₃[–] fields to calculate A_{POT} fields.

A mixed layer model to estimate net CaCO₃ production—The method used to estimate net CaCO₃ production is similar to that used in the previous section to estimate net community production. Net CaCO₃ production in the mixed layer during the warming period of 1990 (CaCO_{3ML-W}), is estimated from changes in the mixed layer A_{POT} inventory corrected for changes due to diffusive A_{POT} flux between the mixed layer and the top of the thermocline:

$$\text{CaCO}_{3\text{ML-W}}|_{\Delta S} = (AH^{S+1}[A_{\text{POT}}^S - A_{\text{POT}}^{S+1}] \times 0.5) + AK_V(dA_{\text{POT}}/dm) \times 0.5, \quad (5)$$

where S denotes season (time step); $[A_{\text{POT}}^S - A_{\text{POT}}^{S+1}]$ is the change in the A_{POT} concentration in the mixed layer; dA_{POT}/dm (mol m⁻⁴) is the vertical A_{POT} gradient between the mixed layer and the upper thermocline; and H and K_V are already defined in the previous section. Note that equation (5) is solved using seasonal mean inputs on each 4° × 5° grid cell in which the mixed layer A_{POT} concentration decreases.

Net change in the mixed layer A_{POT} inventory, $AH^{S+1}[A_{\text{POT}}^S - A_{\text{POT}}^{S+1}] \times 0.5$: Net change in the seasonal mean A_{POT} inventory in the mixed layer is estimated on each grid cell using a derived annual A_{POT} cycle and mixed layer fields. The global decrease in the mixed layer A_{POT} inventory calculated by this method is 0.9 Gt C, which has an error of ±0.2 Gt C resulting from uncertainties of ±5 μmol kg⁻¹ (1 σ) in estimated A_{POT} due to errors in derived regional NA_T/SST algorithms and NO₃⁻ fields. An additional error of ±0.1 Gt C results from uncertainties in the mixed layer depth fields. Thus, the global decrease in the mixed layer A_{POT} inventory during the warming period is subject to an error of up to ±0.3 Gt C.

Diffusive A_{POT} flux, $AK_V(dA_{\text{POT}}/dm) \times 0.5$: The K_V of 0.5 × 10⁻⁴ m² s⁻¹ and regionally varying vertical A_{POT} gradients between the mixed layer and the top of the thermocline are used to estimate the diffusive A_{POT} flux from the upper thermocline. The mean vertical gradients of A_{POT}, which differ in magnitude and sign from those of C_T, range from -0.2 mmol C m⁻⁴ (decreasing concentration with depth) in the subtropical Atlantic Ocean to 0.2 mmol C m⁻⁴ (increasing concentration with depth) in the North Pacific Ocean. The K_V of 0.5 × 10⁻⁴ m² s⁻¹ combined with regional mean vertical A_{POT} gradients gives a global diffusive A_{POT} flux into the mixed layer of <0.1 Gt C, half of it contributes to global net CaCO₃ production and thus is not included in estimating global net CaCO₃ production.

Results

Net community and CaCO₃ production during the warming period—Mass balance of NC_T in the mixed layer gives global estimates of the NC_T inventory decrease of 7.6 and 8.9 Gt C (values in brackets in Table 1), depending on the derived annual NC_T cycles used. Since part of the decrease is due to net CaCO₃ production, the two global estimates are corrected for net CaCO₃ production of 0.9 Gt C as calculated below. Revised global estimates of net community production of 6.7 and 8.0 Gt C represent an 8-month period of 1990 (warming period) and have a probable error of ±2.7

Table 2. Annual rates of regional net CaCO₃ production in the mixed layer (CaCO_{3ML-A}) (Gt C yr⁻¹).

Ocean	Region	Area (×10 ¹² m ²)	CaCO _{3ML-W} * NA _T (Gt C)	Scaling factor†	CaCO _{3ML-A} NA _T (Gt C yr ⁻¹)
Atlantic	40°N–70°N	12.4	0.12	1.25	0.15
	40°N–40°S	49.1	0.14	1.25	0.18
	South of 40°S	18.5	0.08	1.25	0.10
Indian	North of 40°S	43.3	0.08	1.25	0.10
	South of 40°S	23.4	0.10	1.25	0.13
Pacific	40°N–70°N	14.1	0.05	1.25	0.06
	40°N–40°S	119	0.13	1.25	0.16
	South of 40°S	35	0.17	1.25	0.21
Arctic	North of 70°N	2.7	0.02	1.25	0.03
	Global	317.5	0.9		1.1

* Net CaCO₃ production in the mixed layer during the warming period estimated using the mixed layer A_{POT} decrease that are calculated from regional NA_T/SST algorithms and seasonal mean SST and NO₃⁻ fields.

† Scaling factor is a ratio of CaCO₃ fluxes during the warming and cooling period. The value is estimated from multiyear CaCO₃ trap fluxes measured at subarctic central Pacific (49°N, 174°W) between 1990 and 1995 (Takahashi et al. 2000).

Gt C due to an uncertainty of ±2.5 Gt C in the mixed layer NC_T decrease, ±0.4 Gt C in the net air-sea CO₂ flux, and ±0.9 Gt C in the diffusive C_T supply. The probable error is the square root of the sum of the squared errors.

Mass balance of A_{POT} in the mixed layer yields a global net CaCO₃ production of 0.9 Gt C, which also represents an 8-month period of 1990 (Table 2). The global value presented in this paper has an error of ±0.3 Gt C due to an uncertainty of ±0.3 Gt C in the mixed layer A_{POT} decrease.

Scaled-up annual rates of net community and CaCO₃ production—Estimates of global net community production of 6.7 ± 2.7 and 8.0 ± 2.7 Gt C during the warming period must be scaled up to annual rates by including net community production during the 4-month cooling period. The relative amount of sinking particles during the warming and cooling periods can be used to scale up reported values to annual rates if the flux of particles is proportional to net community production. This assumption is a reasonable approximation in much of the oceans.

In the tropical and subtropical oceans, multiyear sediment trap fluxes measured at 150 m in depth near the Hawaii Ocean Time-series (HOT) site (22°N, 158°W) are used to estimate the ratio of particle fluxes during the warming and cooling periods. The annual cycle of vertical export of particulate organic carbon has two pulses: one is centered in late winter and the other in late summer. Between 1988 and 1993, the average rate (C month⁻¹) of particulate organic carbon export during the wintertime is very similar to the summertime rate (Karl et al. 1996). Thus, reported estimates for tropical and subtropical oceans are scaled up by 50% because the warming period is approximately twice the length of the cooling period. Sediment trap data from the Bermuda Atlantic Time-series Study (BATS) site (31°50'N, 64°10'W) are not used in this analysis because there exists

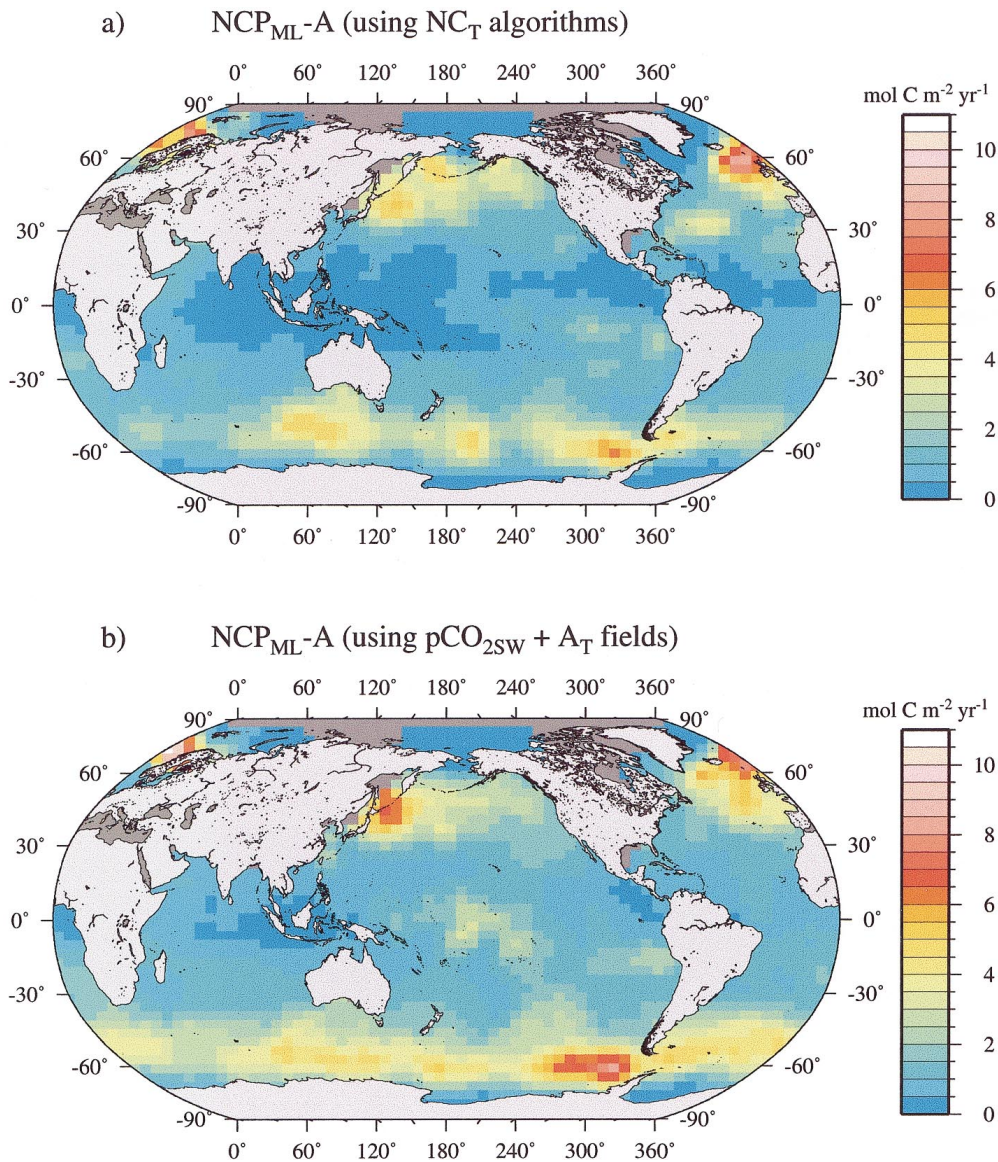


Fig. 3. Annual rates of net community production integrated from the surface to the base of the mixed layer as derived from the cumulative NC_T decrease that is calculated from (a) regional $NC_T/SST/NO_3^-$ algorithms along with seasonal mean SST and NO_3^- fields, and from (b) the pCO_{2SW} and A_T fields using thermodynamic relationships. Values are expressed as $\text{mol C m}^{-2} \text{ yr}^{-1}$. Globally integrated net community production estimates for (a) and (b) are 9.1 (Lee-1) and $10.8 \text{ Gt C yr}^{-1}$ (Lee-2), respectively. Global records of seasonal mean mixed layer depth are interpolated to a $4^\circ \times 5^\circ$ grid cell to match with the grid size used in the pCO_{2SW} climatology.

the significant time lag between net community production and export production (Michaels et al. 1994) and approximately 50% of net community production appears to occur as dissolved organic carbon (Carlson et al. 1994).

In high latitude oceans, two annual cycles of particle fluxes recorded in deep-moored traps at Ocean Weather Station P (50°N , 145°W) of the northeast subarctic Pacific are used to estimate the ratio of particulate organic carbon export during the cooling and warming periods. The average rate of particulate organic carbon export during the summer is two times higher than the rate observed during the winter period (Boyd et al. 1998). This trend is also found in other parts of

the subarctic Pacific (Takahashi et al. 2000). Thus, reported rates of net community production for high latitude waters are increased upward by 25%.

Global extrapolation of these scaling factors obtained from multiyear trap data at two time-series locations gives annual rates of net community production of 9.1 ± 2.7 and $10.8 \pm 2.7 \text{ Gt C yr}^{-1}$ (Fig. 3; see Table 3). Scaled-up annual rates revise global estimates during the warming period upward by about 3 Gt C.

Global net CaCO_3 production of $0.9 \pm 0.3 \text{ Gt C}$ reported here represents extratropical waters with temperatures $<20^\circ\text{C}$ and the upwelled waters in the eastern equatorial

Table 3. Annual rates of regional net community production in the mixed layer (NCP_{ML-A}) ($Gt\ C\ yr^{-1}$).

Ocean	Region	Area ($\times 10^{12}$ m^2)	Scaling factor*	NCP_{ML-A} NC_T ($Gt\ C\ yr^{-1}$)	NCP_{ML-A} $A_T +$ pCO_{2SW} ($Gt\ C\ yr^{-1}$)
Atlantic	40°N–70°N	12.4	1.25	0.80 (0.95)	0.89 (1.04)
	40°N–40°S	49.1	1.50	0.92 (1.09)	0.89 (1.06)
	South of 40°S	18.5	1.25	0.89 (0.99)	1.21 (1.31)
Indian	North of 40°S	43.3	1.50	0.69 (0.79)	0.78 (0.88)
	South of 40°S	23.4	1.25	0.79 (0.91)	1.20 (1.33)
Pacific	40°N–70°N	14.1	1.25	1.23 (1.29)	0.85 (0.91)
	40°N–40°S	119	1.50	2.13 (2.29)	2.79 (2.95)
	South of 40°S	35	1.25	1.44 (1.65)	1.94 (2.15)
Arctic	North of 70°N	2.7	1.25	0.18 (0.20)	0.21 (0.24)
	Global	317.5		9.1[†] (10.2)[‡]	10.8 (11.9)

* Scaling factors are ratios of particulate organic carbon fluxes during the warming and cooling period. The values are obtained from multi-year sediment trap data at the Hawaiian Ocean Time-series (22°N, 158°W) and Ocean Weather Station P (50°N, 145°W) sites.

[†] $NCP_{ML-A} = [NCP_{ML-W}]$ (values in bold in Table 1) \times scaling factor.

[‡] NCP_{ML-A} includes $[CaCO_{3ML-A}]$ (in Table 2).

Pacific (75°W–110°W, 20°N–20°S and 110°W–160°W, 10°N–10°S) during the warming period. Calcification due to coccolithophore and planktonic foraminifera in (sub)tropical waters with temperatures $>20^\circ C$ is assumed to be zero in this analysis because multiyear measurements of surface NA_T in HOT and BATS sites remain constant throughout the year (Bates et al. 1995; Winn et al. 1998) and measured values of NA_T in other oligotrophic oceans are also remarkably invariant (Millero et al. 1998). In extratropical waters, $CaCO_3$ trap fluxes measured in the subarctic central Pacific (49°N, 174°W) between 1990 and 1995 are used to estimate the relative amounts of $CaCO_3$ fluxes during the warming

and cooling seasons (Takahashi et al. 2000). The average rate of $CaCO_3$ export during the summer is approximately two times higher than that observed during the winter. Thus, estimates of net $CaCO_3$ production for extratropical waters are scaled up by 25%. Global extrapolation of this scaling factor yields an annual rate of net $CaCO_3$ production of $1.1 \pm 0.3\ Gt\ C\ yr^{-1}$ for 1990 (Fig. 4).

Discussion

Annual rates of global net community production—Regional patterns of net community production: Estimates of global net community production presented in this paper show different regional patterns in the global oceans. Except for the equatorial upwelling regions in which net community production increases near the equator, it is lowest in areas between 30°N and 30°S (Fig. 3). The low values for these regions can be attributed to small NC_T decreases, as inferred from weaker correlations of NC_T with SST in conjunction with small SST increases. The A_T - pCO_{2SW} based method yields higher values for these regions than the NC_T algorithm-based method (Table 1).

The highest values are found in the western subarctic North Pacific where the cumulative NC_T decrease is largest. The east-west difference in this basin is apparent in the maps constructed from A_T and pCO_{2SW} fields and from derived NC_T algorithms. This zonal difference has been confirmed by sediment trap-based estimates of carbon export (Martin et al. 1987; Boyd et al. 1998; Takahashi et al. 2000) and by satellite-based estimates using seasonal NO_3^- drawdown derived from a basin-scale NO_3^-/SST relationship and satellite-derived SST data (Goes et al. 2000). Seasonally well-sampled pCO_{2SW} data in this basin provide an additional line of evidence supporting this zonal difference. Takahashi et al. (1993) reported that the pCO_{2SW} in the northwestern North

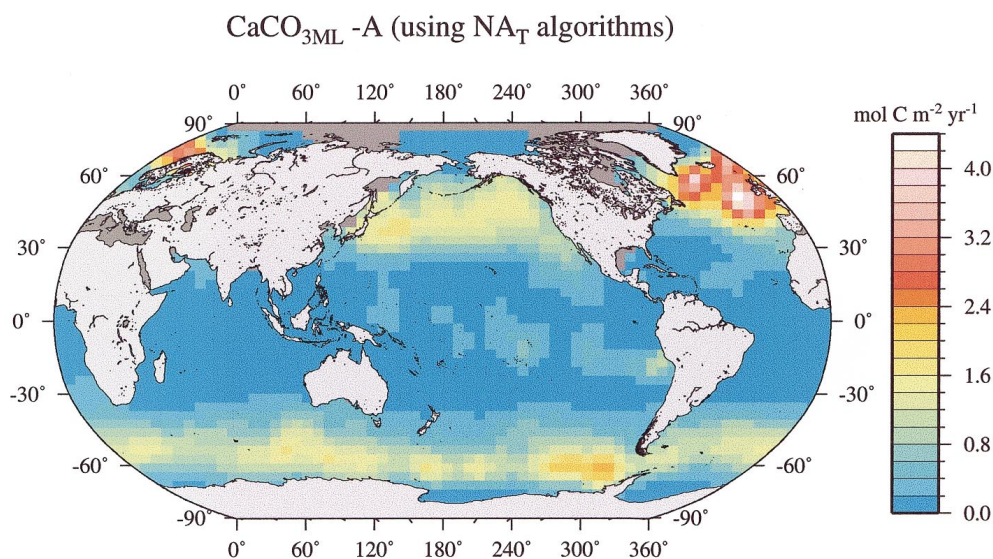


Fig. 4. Annual rate of net $CaCO_3$ production integrated from the surface to the base of the mixed layer as derived from the magnitude of seasonal NA_{POT} decrease calculated from regional NA_T/SST algorithms and seasonal mean SST and NO_3^- fields. Values are expressed as mole $C\ m^{-2}\ yr^{-1}$. Globally integrated net $CaCO_3$ production for 1990 is $1.1\ Gt\ C\ yr^{-1}$.

Pacific varies seasonally by $160 \mu\text{atm}$, whereas the $\text{pCO}_{2\text{sw}}$ in the northeastern North Pacific varies by $40 \mu\text{atm}$. Estimated values for the Southern Ocean and the North Atlantic are lower than those for the western subarctic Pacific due primarily to a smaller magnitude of seasonal NC_T decrease.

Comparison with independent estimates based on time-series measurements: The accuracy of the estimates reported in this paper can be assessed by comparing them with results from time-series observations of various geochemical tracers. The annual rates of net community production at the HOT site are 2.7 ± 1.7 , 1.6 ± 0.9 , and $2.0 \pm 0.9 \text{ mol C m}^{-2} \text{ yr}^{-1}$, which were estimated by using mass balances of the mixed layer dissolved O_2 , inorganic stable carbon isotope ($\delta^{13}\text{C}$), and organic carbon, respectively (Emerson et al. 1997). These estimates are in good agreement with the values presented here of 1.7 ± 0.7 to $2.2 \pm 0.5 \text{ mol C m}^{-2} \text{ yr}^{-1}$, obtained from $A_T\text{-pCO}_{2\text{sw}}$ fields and regional NC_T algorithms, respectively, for several grid cells near the HOT site. There is also broad agreement between the estimates presented in this paper of 2.6 to $3.5 \text{ mol C m}^{-2} \text{ yr}^{-1}$ and the values of 3 to $4 \text{ mol C m}^{-2} \text{ yr}^{-1}$ (Jenkins and Wallace 1992), which were obtained by measuring the vertical integral of the O_2 utilization rates, O_2 production rate in the euphotic zone, and upward flux of NO_3^- near the BATS site.

Comparison with other global estimates: Existing estimates of global net community production (or new and export production) using independent methods range from as low as 3.4 Gt C yr^{-1} (Eppley and Peterson 1979) to as high as $21.9 \text{ Gt C yr}^{-1}$ (Packard et al. 1988). The global export/new production using a pelagic food web model and empirical models ranges from 11 to 21 Gt C yr^{-1} (Laws et al. 2000). In contrast, estimates of export production based on extrapolation of shallow sediment trap fluxes are 3.4 (Eppley and Peterson 1979) and 7.3 Gt C yr^{-1} (Martin et al. 1987). A geochemical approach using seasonal efflux of O_2 across the air-sea interface yields a global net community production of 6.7 Gt C yr^{-1} if scaled to a O_2 :C ratio of 1.45 (Louanchi and Najjar 2000). Estimates of net community production using the seasonal drawdown of nitrate (NO_3^-) and phosphate (PO_4^{2-}) coupled with Redfield ratio conversions are 4.6 and 5.3 Gt C yr^{-1} , respectively (Louanchi and Najjar 2000).

For comparison between various estimates, geochemical estimates using mass balances of O_2 , NO_3^- , and PO_4^{2-} in the mixed layer should be scaled up to annual rates by accounting for net community production during the cooling season. The steady state assumption should also be made for comparison because net community production would be equal to export and new productions only in the steady state. Global estimates from this study are compared with results from two recent studies by Laws et al. (2000) and Louanchi and Najjar (2000) (Fig. 5). The global net community production estimates of 9.1 ± 2.7 and $10.8 \pm 2.7 \text{ Gt C yr}^{-1}$, henceforth referred to as "Lee-1" and "Lee-2," respectively, are in good agreement with the value of 9.4 Gt C yr^{-1} determined from the net efflux of biologically produced O_2 (Louanchi and Najjar 2000). Louanchi and Najjar's value has revised Najjar and Keeling's O_2 -based estimate upward by $4\text{--}5 \text{ Gt}$

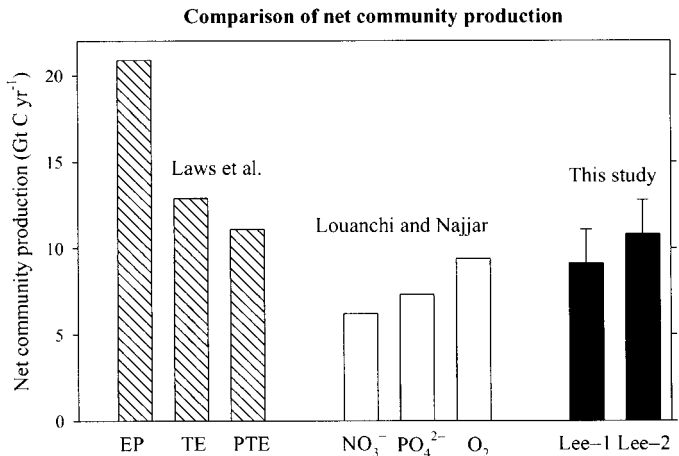


Fig. 5. Comparison of annual rates of global net community production. The values from this study are compared with those of Laws et al. (2000) and with scaled-up estimates of Louanchi and Najjar (2000). Lee-1 and Lee-2 represent global net community production as shown in Figs. 2a and 2b, respectively. Error bars for Lee-1 and Lee-2 are obtained from uncertainties involved in solving Eq. 3. For an absolute comparison between the independent estimates, Louanchi and Najjar's estimates of 4.6 , 5.3 , and 6.7 Gt C yr^{-1} representing the warming period are scaled up to an annual rate of 6.2 , 7.3 , and 9.4 Gt C yr^{-1} , respectively. Louanchi and Najjar's estimates for (sub)tropical and high latitude waters are increased by 50 and 25% , respectively.

C by including the tropics between 20°N and 20°S and net community production occurring during the cooling season. Lee-1 and Lee-2 are higher than the values of 6.2 and 7.3 Gt C yr^{-1} , which are determined from seasonal drawdown of NO_3^- and PO_4^{2-} , respectively (Louanchi and Najjar 2000). Scaled-up global values based on NO_3^- and PO_4^{2-} account for wintertime net community production and are about 35% higher than those originally obtained by Louanchi and Najjar (2000). Lee-1 and Lee-2 are similar in magnitude with Laws et al.'s estimates of 11.1 and $12.9 \text{ Gt C yr}^{-1}$, which are based on the pelagic food web (PTE) and the temperature-export (TE) models, respectively. The former maximizes the ability of the system to return to the steady state following the perturbation, whereas the latter relates export production/total production ratios to temperature. However, the values presented here are significantly lower than Laws et al.'s value of 21 Gt C yr^{-1} using the Eppley-Peterson (EP) model, which relates export production/total production ratios to total production. A more detailed description of the models is given in Laws et al. (2000).

There is sharp contrast in regional comparisons, although Lee-1 and Lee-2 are comparable with $11.1 \text{ Gt C yr}^{-1}$ calculated by using the PTE model (Fig. 6). Laws et al.'s estimate for the Atlantic is much larger than Lee-1 and Lee-2 for the same basin. For the Southern Ocean south of 50°S , three tracer-based estimates (PO_4^{2-} , O_2 and NC_T) are in good agreement but are twice the magnitude of the Laws et al.'s estimate. Overall, Lee-1 and Lee-2 are most consistent with the O_2 -based estimate in regional comparisons.

Causes for discrepancies: The difference between net community production presented in this paper and those de-

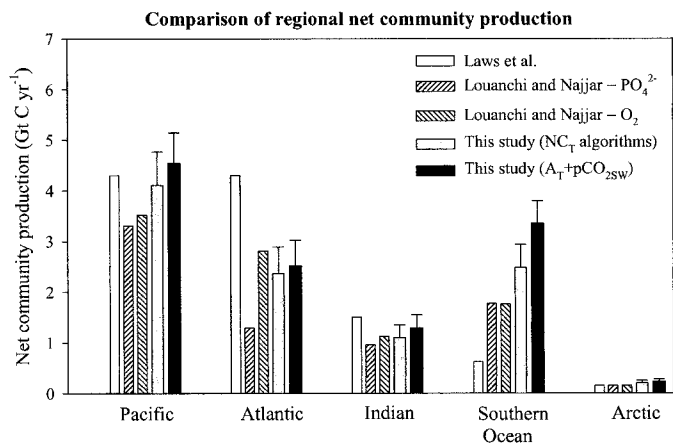


Fig. 6. Comparison of regional net community production estimates. The values from this study are compared with those of Laws et al. (2000) and with scaled-up estimates of Louanchi and Najjar (2000). For comparison, Laws et al.'s regional rates calculated from the global rate of 11.2 Gt C yr⁻¹ are used. Results are summed over five regions as defined in Laws et al.: the Atlantic (50°S–70°N), the Indian (north of 50°S), the Pacific (50°S–70°N), the Southern Ocean (south of 50°S), and the Arctic (north of 70°N). Error bars for Lee-1 and Lee-2 are obtained from uncertainties involved in solving Eq. 3 for each oceanic region.

terminated from other studies could be caused by several factors. The NO₃⁻-based value might be significantly underestimated in (sub)tropical waters where the fixation of atmospheric nitrogen can support up to half of the net community production (Karl et al. 1997). Despite the overall consistency of the O₂-based estimate with Lee-1 and Lee-2, significant improvement can be achieved by accurate parameterization of gas exchange velocity (Najjar and Keeling 2000). Laws et al.'s estimates might also be subject to errors due to insufficient understanding of the factors that govern export production/total production ratios (Laws et al. 2000).

Lee-1 and Lee-2 could be underestimated because vertical advection of subsurface waters with high NC_T during the warming period counteracts the mixed layer NC_T decrease caused by net community production. Lee-1 and Lee-2 do not account for net community production occurring below the seasonal mixed layer, which is particularly important in areas where primary production extends to greater depths due to deeper light penetration. Derived regional NC_T algorithms may not capture the full effect of mesoscale net community production that results from eddy pumping of nutrients injected into the euphotic zone (McGillicuddy et al. 1998). Lee-1 and Lee-2 are further underestimated because they do not include net community production occurring in coastal regions in which primary production and new production/total production ratios are high (Eppley and Peterson 1979).

The difference in various estimates could be partially explained if there is interannual variability in net community production. For instance, the estimates presented here represent 1990, whereas Laws et al.'s estimates based on the PTE model represent the period from October 1997 to September 1998. It is presently not possible to prove whether there is a difference in global net community production

between 1990 and 1998. However, multiyear sediment trap data collected at the HOT (Karl et al. 1996) and the subarctic north Pacific sites (Takahashi et al. 2000) show that the annual rate of export production varies as much as 100% from year to year.

Global net CaCO₃ production—Regional patterns of net CaCO₃ production: Estimated net CaCO₃ production is virtually zero for waters with temperature >20°C in (sub)tropical areas between 30°N and 30°S except in the equatorial upwelling regions where it increases near the equator (Fig. 4). Near zero values can be attributed to a remarkably constant NA_T concentration throughout the year (Bates et al. 1995; Winn et al. 1998). Higher values in sub-polar waters can be attributed to larger NA_T drawdown as inferred from stronger correlations of NA_T with SST. The net CaCO₃ production for a given area in the North Pacific (>30°) is lower than in the North Atlantic, which supports the long-held contention that ballasting of exported organisms by CaCO₃ is more important in the North Atlantic than in the North Pacific (Berger 1992).

Comparison with estimates from other studies: Existing global estimates of net CaCO₃ production are based on models that combine information about ocean circulation with variations in A_{POT}, which is corrected for fresh water fluxes and recycled nitrogen. Various models yield global estimates ranging from 0.5 to 1.5 Gt C yr⁻¹ (see Milliman et al. 1999). However, the models are simply tuned to the global mean A_{POT} profile, which means that the spatial distribution of net CaCO₃ production is poorly constrained. Note that net community production estimated using these models is 3 to 5 Gt C yr⁻¹, which is on the low side of current estimates, which suggests that the model-derived net CaCO₃ production may be low as well.

Global net CaCO₃ production of 1.1 ± 0.3 Gt C yr⁻¹ reported in this paper falls within a range of existing estimates. However, various model-based estimates are nearly two to three times higher than those measured by sediment traps that are typically moored at depths well below the mixed layer to minimize turbulent mixing and horizontal advection. Milliman et al. (1999) suggests that the discrepancy may be due to biologically mediated dissolution of CaCO₃ above the lysocline. Conclusive evidence is needed before the view of the conservative nature of pelagic carbonate at shallow ocean depths can be modified. Regional comparisons are not possible at the present time because none of the existing global estimates provides regional values.

Causes for discrepancies: The estimate of 1.1 Gt C yr⁻¹ is likely to be a lower limit because it does not include net CaCO₃ production occurring in coastal regions and account for vertical advection of subsurface waters with high A_{POT} during the warming period. Vertical advection of subsurface waters with higher A_{POT} values counteracts the mixed layer A_{POT} decrease resulting from net CaCO₃ production in the mixed layer.

Conclusion

Global net community production of 6.7 and 8.0 Gt C has been estimated, for the first time, from the mass balance of the NC_T concentration in the mixed layer. These estimates are almost certainly low, as net community production during the cooling period is not included and coastal waters are believed to account for significant net community production. By including wintertime net community production deduced from multiyear sediment trap data at the HOT and Ocean Weather Station P sites, estimates of global net community production during the warming period are scaled up to 9.1 and 10.8 Gt C yr⁻¹, which could be close to annual rates of global net community production in the mixed layer.

References

- BATES, N. R., A. F. MICHAELS, AND A. H. KNAP. 1995. Alkalinity changes in the Sargasso Sea: Geochemical evidence of calcification? *Mar. Chem.* **51**: 347–358.
- BERGER, W. H. 1992. Global map of ocean productivity, p. 429–455. *In* W. H. Berger, V. S. Smetacek, and G. Wefer [eds.], *Productivity of the Ocean: Present and Past*. Wiley.
- , K. FISCHER, C. LAI, AND G. WU. 1987. Ocean productivity and organic carbon flux. Part I. Overview and maps of primary production and export production. University of California, San Diego. SIO Reference 87-30.
- BOYD, P., C. S. WONG, J. MERRILL, F. WHITNEY, J. SNOW, P. J. HARRISON, AND J. GOWER. 1998. Atmospheric iron supply and enhanced vertical carbon flux in the NE subarctic Pacific: Is there a connection? *Glob. Biogeochem. Cycles* **12**: 429–441.
- BREWER, P. G., G. T. F. WONG, M. P. BACON, AND D. W. SPENCER. 1975. An oceanic calcium problem? *Earth Planet. Sci. Lett.* **26**: 81–87.
- CARLSON, C. A., H. W. DUCKLOW, AND A. F. MICHAELS. 1994. Annual flux of dissolved organic carbon from the euphotic zone in the northwestern Sargasso Sea. *Nature* **371**: 405–408.
- CONKRIGHT, M. E., T. O'BRIEN, S. LEVITUS, T. P. BOYER, J. ANTONOV, AND C. STEPHENS. 1998. World Ocean database 1998, CD-ROM Data Set Documentation, Natl. Oceanogr. Data Cent. Int. Rep. 14.
- CONWAY, T. J., P. P. TANS, L. S. WATERMAN, K. W. THONING, D. R. KITZIS, K. A. MASARIE, AND N. ZHANG. 1994. Evidence for interannual variability of the carbon cycle from the National Oceanic and Atmospheric Administration/Climate Monitoring and Diagnostics Laboratory Global Air Sampling Network. *J. Geophys. Res.* **99**: 22831–22855.
- DENMAN, K. L., AND M. MIYAKE. 1973. Upper layer modification at Ocean Station Papa: Observations and simulation. *J. Phys. Oceanogr.* **3**: 185–196.
- DICKSON, A. G., AND F. J. MILLERO. 1987. A comparison of the equilibrium constants for the dissociation of carbonic acid in seawater media. *Deep-Sea Res.* **34**: 1733–1743.
- DUGDALE, R. C., AND J. J. GOERING. 1967. Uptake of new and regenerated forms of nitrogen in primary productivity. *Limnol. Oceanogr.* **12**: 196–206.
- EMERSON, S., P. QUAY, D. KARL, C. WINN, L. TUPAS, AND M. LANDRY. 1997. Experimental determination of the organic carbon flux from open-ocean surface waters. *Nature* **389**: 951–954.
- EPPLEY, R. W., AND B. J. PETERSON. 1979. Particulate organic matter flux and planktonic new production in the deep ocean. *Nature* **282**: 677–680.
- FALKOWSKI, P. G., R. T. BARBER, AND V. SMETACEK. 1998. Biogeochemical controls and feedbacks on ocean primary production. *Science* **281**: 200–206.
- GOES, J. I., T. SAINO, H. OAKU, J. ISHIZAKA, C. S. WONG, AND Y. NOJIRI. 2000. Basin scale estimates of sea surface nitrate and new production from remotely sensed sea surface temperature and chlorophyll. *Geophys. Res. Lett.* **27**: 1263–1266.
- JENKINS, W. J., AND J. C. GOLDMAN. 1985. Seasonal oxygen cycling and primary production in the Sargasso Sea. *J. Mar. Res.* **43**: 465–491.
- , AND D. W. R. WALLACE. 1992. Tracer based inferences of new production in the sea, p. 317–332. *In* P. G. Falkowski and A. D. Woodhead [eds.], *Primary productivity and biogeochemical cycles in the Sea*. Plenum.
- KALNAY, E., AND OTHERS. 1996. The NCEP/NCAR 40-year reanalysis project. *Bull. Amer. Meteor. Soc.* **77**: 437–471.
- KARL, D. M., J. R. CHRISTIAN, J. E. DORE, D. V. HEBEL, R. M. LETELIER, L. M. TUPAS, AND C. D. WINN. 1996. Seasonal and interannual variability in primary production and particle flux at station ALOHA. *Deep-Sea Res.* **43**: 539–568.
- , R. LETELIER, L. TUPAS, J. DORE, J. CHRISTIAN, AND D. HEBEL. 1997. The role of nitrogen fixation in biogeochemical cycling in the subtropical North Pacific Ocean. *Nature* **388**: 533–538.
- LAWS, E. A., P. G. FALKOWSKI, W. O. SMITH, J. R. H. DUCKLOW, AND J. J. MCCARTHY. 2000. Temperature effects on export production in the open ocean. *Glob. Biogeochem. Cycles* **14**: 1231–1246.
- LEDWELL, J. R., A. J. WATSON, AND C. S. LAW. 1993. Evidence for slow mixing across the pycnocline from an open-ocean tracer-release experiment. *Nature* **364**: 701–703.
- LEE, K., R. H. WANNINKHOF, R. A. FEELY, F. J. MILLERO, AND T.-H. PENG. 2000. Global relationships of total inorganic carbon with temperature and nitrate in surface water. *Glob. Biogeochem. Cycles* **14**: 979–994.
- LOUANCHI, F., AND R. G. NAJJAR. 2000. A global monthly climatology of phosphate, nitrate, and silicate in the upper ocean: Spring-summer export production and shallow remineralization. *Glob. Biogeochem. Cycles* **14**: 957–977.
- MARTIN, J. H., G. A. KNAUER, D. M. KARL, AND W. W. BROENKOW. 1987. VERTEX: carbon cycling in the northeast Pacific. *Deep-Sea Res.* **34**: 267–285.
- MCGILLICUDDY, D. J., AND OTHERS. 1998. Influence of mesoscale eddies on new production in the Sargasso Sea. *Nature* **394**: 263–266.
- MEHRBACH, C., C. H. CULBERSON, J. E. HAWLEY, AND R. M. PYTKOWICZ. 1973. Measurements of the apparent dissociation constants of carbonic acid in seawater at atmospheric pressure. *Limnol. Oceanogr.* **18**: 897–907.
- MICHAELS, A. F., N. R. BATES, K. O. BUESSELER, C. A. CARSON, AND A. H. KNAP. 1994. Carbon-cycle imbalance in the Sargasso Sea. *Nature* **372**: 537–540.
- MILLERO, F. J., K. LEE, AND M. ROCHE. 1998. Distribution of alkalinity in the surface waters of the major oceans. *Mar. Chem.* **60**: 111–130.
- MILLIMAN, J. D., P. J. TROY, W. M. BALCH, A. K. ADAMS, Y.-H. LI, AND F. T. MACKENZIE. 1999. Biologically mediated dissolution of calcium carbonate above the chemical lysocline. *Deep-Sea Res.* **46**: 1653–1669.
- MONTEREY, G., AND S. LEVITUS. 1997. Seasonal variability of mixed layer depth for the world ocean. NOAA Atlas NRS DIS 14. U.S. Gov. Printing Office.
- MUNK, W. H. 1966. Abyssal recipes. *Deep-Sea Res.* **13**: 707–730.
- NAJJAR, R. G., AND R. F. KEELING. 2000. Mean annual cycle of the air-sea oxygen flux: A global view. *Glob. Biogeochem. Cycles* **14**: 573–584.
- PACKARD, T. T., M. DENIS, M. RODIER, AND P. GARFIELD. 1988.

- Deep ocean metabolic CO₂ production: Calculations from ETS activity. *Deep-Sea Res.* **35**: 371–382.
- TAKAHASHI, K., N. FUJITANI, M. YANADA, AND Y. MAITA. 2000. Long-term biogenic fluxes in the Bering Sea and the central subarctic Pacific Ocean. *Deep-Sea Res.* **47**: 1723–1759.
- TAKAHASHI, T., R. A. FEELY, R. F. WEISS, R. WANNINKHOF, D. W. CHIPMAN, S. C. SUTHERLAND, AND T. TAKAHASHI. 1997. Global air-sea flux of CO₂: An estimate based on measurements of sea-air pCO₂ difference. *Proc. Natl. Acad. Sci. U.S.A.* **94**: 8292–8299.
- , J. OLAFSSON, J. G. GODDARD, D. W. CHIPMAN, AND S. C. SUTHERLAND. 1993. Seasonal variation of CO₂ and nutrients in the high-latitude surface oceans: A comparative study. *Glob. Biogeochem. Cycles* **7**: 843–878.
- WANNINKHOF, R. 1992. Relationship between wind speed and gas exchange over the Ocean. *J. Geophys. Res.* **97**: 7373–7382.
- WINN, C. D., Y.-H. LI, F. T. MACKENZIE, AND D. M. KARL. 1998. Rising surface ocean dissolved inorganic carbon at the Hawaii Ocean Time-series site. *Mar. Chem.* **60**: 33–47.

Received: 11 December 2000

Accepted: 23 April 2001

Amended: 15 May 2001